Trends and Scales of Observed Soil Moisture Variations in China

NIE Suping[*1,2] (聂肃平), LUO Yong[3] (罗 勇), and ZHU Jiang[1] (朱 江)

[1]*Institute of Atmospheric Physics, Chinese Academy of Sciences, Beijing* 100029

[2]*Graduate University of Chinese Academy of Sciences, Beijing* 100049

[3]*National Climate Center, China Meteorological Administration, Beijing* 100081

ABSTRACT

A new soil moisture dataset from direct gravimetric measurements within the top 50-cm soil layers at 178 soil moisture stations in China covering the period 1981–1998 are used to study the long-term and seasonal trends of soil moisture variations, as well as estimate the temporal and spatial scales of soil moisture for different soil layers. Additional datasets of precipitation and temperature difference between land surface and air (TDSA) are analyzed to gain further insight into the changes of soil moisture. There are increasing trends for the top 10 cm, but decreasing trends for the top 50 cm of soil layers in most regions. Trends in precipitation appear to dominantly influence trends in soil moisture in both cases. Seasonal variation of soil moisture is mainly controlled by precipitation and evaporation, and in some regions can be affected by snow cover in winter. Timescales of soil moisture variation are roughly 1–3 months and increase with soil depth. Further influences of TDSA and precipitation on soil moisture in surface layers, rather than in deeper layers, cause this phenomenon. Seasonal variations of temporal scales for soil moisture are region-dependent and consistent in both layer depths. Spatial scales of soil moisture range from 200–600 km, with topography also having an affect on these. Spatial scales of soil moisture in plains are larger than in mountainous areas. In the former, the spatial scale of soil moisture follows the spatial patterns of precipitation and evaporation, whereas in the latter, the spatial scale is controlled by topography.

1. Introduction

Soil moisture is an important variable in the climate system. It governs energy and water exchanges at the land-air boundary and controls interactions between land surface and atmosphere. It is very important both in terms of its influence on the climate system and for its impact on future climate change (Srinivasan et al., 2000). Many studies related to soil moisture and climate have been carried out recently. Various modeling studies (Shukla and Mintz, 1982; Koster and Suarez, 1995, 1996) have shown that persistent anomalies of soil moisture have tremendous influence on the climate, especially in the tropics and the summer hemisphere extratropics. Using GCM simulations, Koster et al. (2000, 2004) also found that land surface moisture state contributes significantly to precipitation predictability in transition zones between dry and humid climates. Timbal et al. (2002) found that forecasting skill is crucially dependent on soil moisture variability over the continent. Dirmeyer (2000) found that Global Soil Wetness Project (GSWP) soil moisture led to improved simulations of rainfall patterns globally, and the improvements were particularly marked over monsoonal Asia.

However, long-term records of soil moisture are not available in many parts of the world. The Global Soil Moisture Data Bank (Robock et al., 2000), fortunately, contains substantial soil moisture observation data, mainly for Asia. Robock et al. (1995, 1997, 1998), Schlosser et al. (1997, 2000) and Entin et al. (1999) used these soil moisture data to evaluate soil moisture simulations in land surface models.

For the correct interpretation of such model/observation comparisons results, it is important to know the statistical structure of the soil moisture field. The

*Corresponding author: NIE Suping, niesuping@mail.iap.ac.cn

long-term and seasonal trends of soil moisture variations are important for providing accurate climate background and the initial state of soil moisture in land surface models. Studying the scales of soil moisture variations is also very important for understanding patterns of climate change (Shinoda and Yamaguchi, 2003; Dai et al., 2004), designing soil moisture observation networks (Vinnikov et al., 1999a,b), and understanding many aspects of weather (Fast and McCorcle, 1991; van den Hurk et al., 1997).

Analyzing soil moisture scales can help explain the proportion of soil moisture variation contributing to small-scale, short-term influences, as well as large-scale, long-term influences. Vinnikov et al. (1996) developed a statistical model based on the theory of Delworth and Manabe (1988) of temporal and spatial variations of soil moisture. They divided the variations into red noise and white noise components. Using Russian soil moisture observations, it was found that the red noise component of temporal and spatial variability represented most of the soil moisture variance and reflected the statistical properties of the monthly averaged precipitation field, while there was a certain amount of small-scale variability related to soil texture, topography, vegetation, and root structure. Entin et al. (2000) extended this analysis using soil moisture observations from Illinois (USA), Mongolia, Russia, and China. They showed that there was a timescale of roughly 2–3 months and a spatial scale of 500 km in all these regions for both the top 10-cm and top 100-cm layers.

The Chinese dataset in the Global Soil Moisture Data Bank, however, only consists of 40 soil moisture stations. As China spans such a large geographical area and covers many kinds of climate regions, such as the continental monsoon zone, plane-humid zone, mountain-humid zone, and semiarid zone, this really is a relatively small number of stations and it makes it difficult to conduct detailed analyses of soil moisture variations in different geographical regions of the country. A detailed study of soil moisture in China could provide opportunities for the fine analysis of the influences of soil moisture in different climate areas. Due to the lack of soil moisture observations, particularly long-term soil moisture data, few studies on the variations and scales of soil moisture in China have been conducted recently. Entin et al. (1999, 2000) used soil moisture data of 78 stations (mainly located in the east of China); Li et al. (2005) used data from 43 stations in China; and Liu et al. (2001) used 99 stations, but with a short period series of only two years to carry out their research. The datasets used were not sufficient for a fine analysis of soil moisture in China.

In this paper, the statistical structure and the scales of temporal and spatial variation of soil moisture in China are studied using a new soil moisture dataset covering a large area of the country. This dataset is the most intact soil moisture data that can be obtained in China. It also has the longest time series (from 1981 to 1998) among existing soil moisture datasets in China. Presently, the dataset has been previously used only by Zhang et al. (2004), for the primary analysis of vertical characteristics at 57 stations. There is, therefore, a good opportunity for a detailed study of the inherent characteristics of soil moisture variations in China.

The data used in this study is described in section 2; long-term trends and seasonal variations are analyzed in section 3; temporal scales and spatial scales are discussed in sections 4 and 5 respectively; and the final section presents a discussion and conclusions.

2. Data

The soil moisture dataset used in this paper was obtained from the National Meteorological Information Center of the China Meteorological Administration. The data were observed during 18 years from 1981 to 1998, at 178 soil moisture stations across China. Not all the soil moisture stations are located under the same climate states. Around 55 agrometeorological stations were irrigated during growing seasons, while others were under the influence of the natural climate state. In order to study natural characteristics of soil moisture in China, only the data of stations in non-irrigated areas are used in this paper. For the convenience of discussion, these stations are subdivided into five regions based on topography and climatology. Data availability is also considered. Figure 1 shows the location of the 178 soil moisture stations and the distribution of the five geographical regions.

Regions 1 and 2 are subhumid zones. Sixty percent of region 1 is mountainous and covered by evergreen coniferous and broadleaved mixed forest; and forty percent is plain, mostly covered by grassland and agricultural fields. More than 85% of region 2 is plain and the rest is hilly. The soils are mainly dark brown and chernozem in region 1 and brunisolic in region 2. Region 3 is a semiarid plateau of mountains and hills covered by scrubland and steppe. The soil is mostly cultivated loessial soil. Region 4 is a main agricultural area of China, with a typical subhumid and temperate climate. More than 90% of this region is plain and the soil is mostly brown loam. Region 5 is the Yunnan-Guizhou Plateau zone, which features the most mountains and the highest altitude of all five regions. This region has a typical mountain-humid climate. The soil is mainly red and yellow loam and the vegetation is mainly subtropical evergreen broadleaf forest.
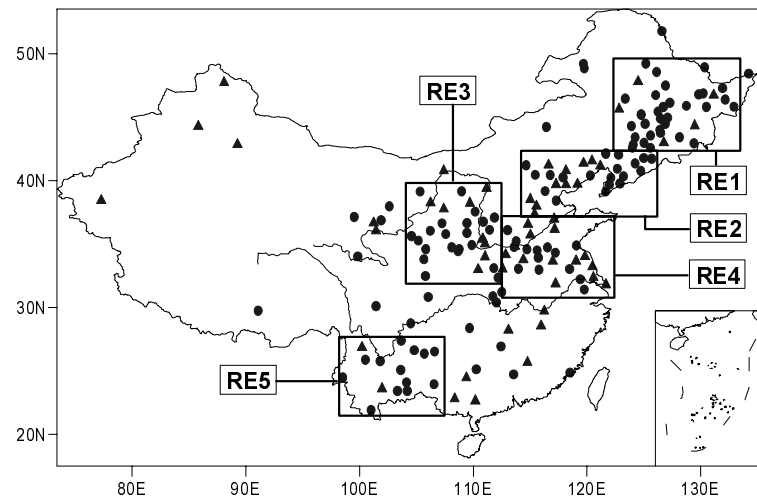
Fig. 1. Map of China soil moisture stations and distribution of the five regions. Circles and triangles represent non-irrigated stations and irrigated stations respectively. Regions 1 and 2 are subhumid zones. Region 3 is a semiarid mountain plateau zone. Region 4 is an agricultural zone. Region 5 is the Yunnan-Guizhou Plateau zone.

Table 1. The number of non-irrigated soil moisture stations, soil moisture stations which had native states and more than 10 years of data (asterisk numbers), precipitation and TDSA in regions 1 to region 5.

| Numbers of stations	Region 1	Region 2	Region 3	Region 4	Region 5
Soil moisture	25^*	10^*	13^*	17^*	9^*
	33	20	22	15	13
Precipitation	52	64	69	73	82
TDSA	52	64	67	73	82

The five regions include 103 non-irrigated soil moisture stations in all. Other stations are not considered due to sparse distributions in space. Table 1 presents the numbers of non-irrigated soil moisture stations and the numbers of stations which had more than 10 years data during the 18-year dataset period for each region. At all stations, soil moisture observations were quantified gravimetrically, which involves removing a core of soil and dividing it into different layers, taking a sample from each layer to be weighed, heated to evaporate all the water in the soil, and then weighed again. The difference between the two weights provides a measure of soil water content. Soil moisture at these stations was measured in 11 vertical layers: 5-cm layers form 0–10 cm, and 10-cm layers form 10–100 cm. Most of the stations did not have observations for beneath 50 cm, and so only 0–50-cm layers were used in this study. Soil moisture was routinely measured three times per month on the 8th, 18th, and 28th, at all stations. However, observations would be delayed or cancelled as a result of precipitation. In the north of China, stations cancelled soil moisture observations during the freezing season. Some stations performed additional observations on the 3rd, 13th and 23rd in certain months. For obtaining a standard time series to evaluate the autocorrelation of soil moisture, the dataset was binned in time. The method of setting up bins is similar to that of Entin et al. (2000).

Precipitation is a random forcing for the land surface and the storage of precipitation in soil can increase soil water content. Evaporation is a persistent process on the land surface, which can release soil water back into the atmosphere and cause a decrease in soil water content. These two factors have important influences on changes in and patterns of soil moisture (Cayan and Georgakakos, 1995). Without data of observed evaporation, the influence of evaporation on soil moisture cannot be evaluated directly. However, with an approximate relationship to temperature difference between land surface and air (hereafter denoted as TDSA), the influence of evaporation on soil moisture can be studied. Three datasets of precipitation, land surface temperature, and air temperature are used in this paper to analyze the mechanisms underlying changes in soil moisture. TDSA is calculated from land surface temperature and air temperature. Obser-
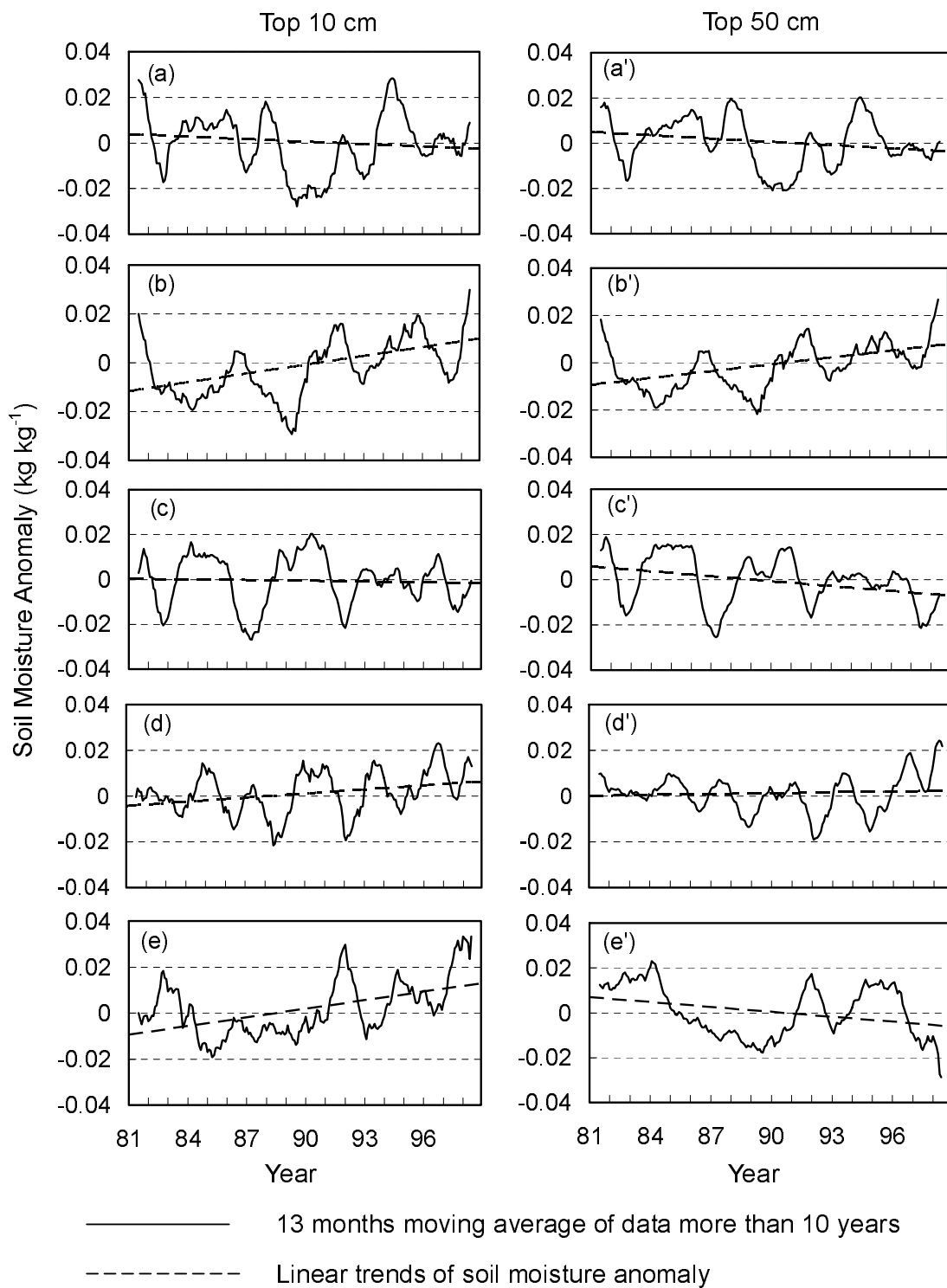
Fig. 2. Interannual variabilities and linear trends of soil moisture in (a) and (a') region 1, (b) and (b') region 2, (c) and (c') region 3, (d) and (d') region 4, and (e) and (e') region 5. Thick solid lines represent a 13-month binomial filter of regional-mean soil moisture anomaly (kg kg^{-1}), calculated with non-irrigated stations with more than 10 years worth of data. Dashed lines represent linear trends of soil moisture anomaly during 1981–1998. The left column represents the top 10-cm soil layer, and the right column represents the top 50-cm soil layer.

Precipitation   TDSA
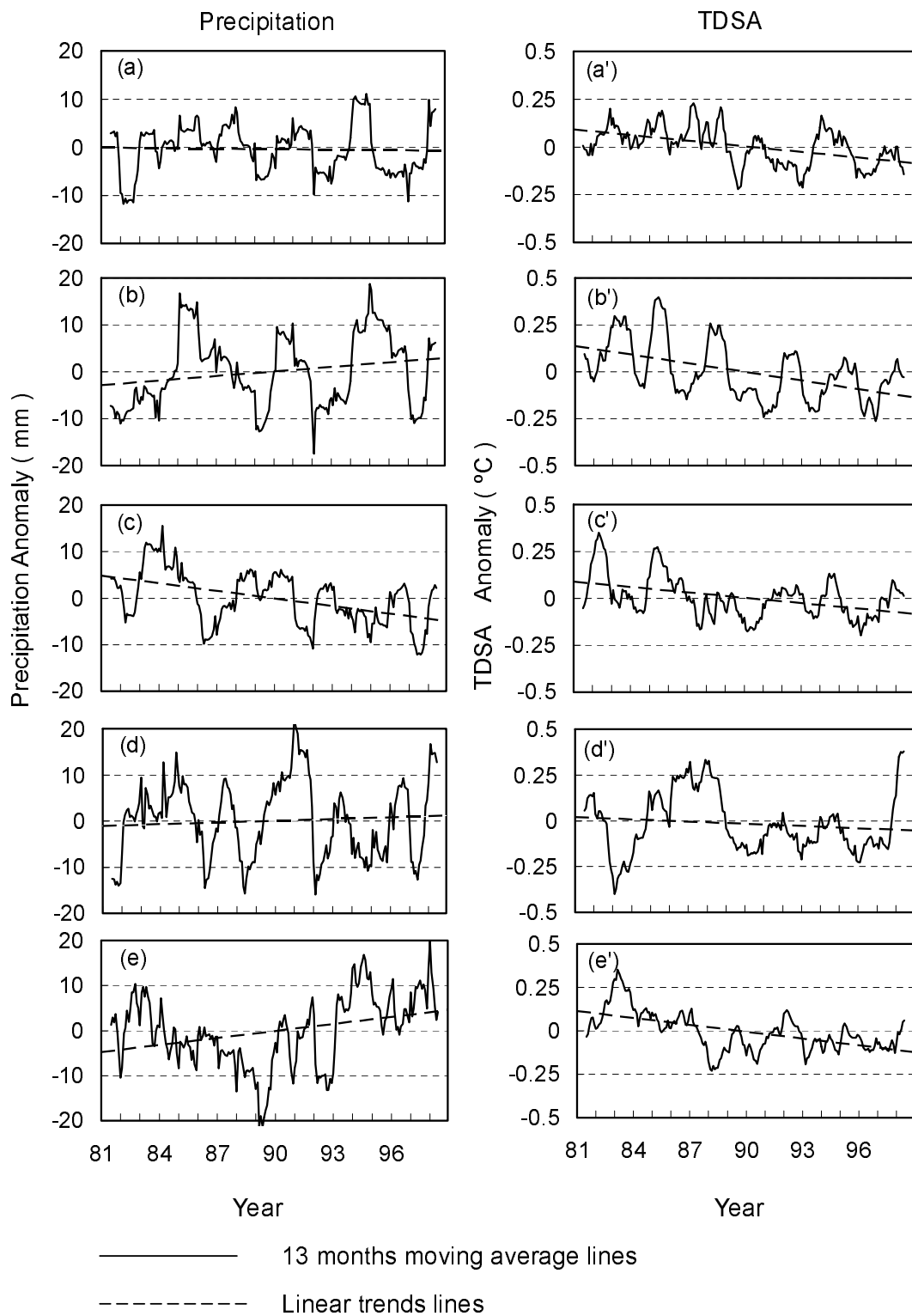
Fig. 3. Interannual variabilities and linear trends of precipitation and TDSA in (a) and (a') region 1, (b) and (b') region 2, (c) and (c') region 3, (d) and (d') region 4, and (e) and (e') region 5. Thick solid lines represent a 13-month binomial filter of interannual variabilities of regional-mean precipitation anomaly (mm) and TDSA anomaly (°C) from region 1 to region 5 of China during the period 1981–1998. Dashed lines represent linear trends of precipitation anomaly and TDSA anomaly. The left column represents the precipitation, and the right column represents the TDSA.

Table 2. Linear trend coefficients of soil moisture, precipitation and TDSA in the period 1981–1998 for the five regions. Bold typeface means the trends are significant at the 99% confidence level.

	Soil moisture (kg kg^{-1} yr^{-1})		Precipitation (mm yr^{-1})	TDSA ($^{\circ}$C yr^{-1})
	Top 10 cm	Top 50 cm		
Region 1	-0.00036	-0.00048	-0.04	-0.0096
Region 2	0.00120	0.00096	0.32	-0.0156
Region 3	-0.00011	-0.00072	-0.55	-0.0096
Region 4	0.00060	0.00012	0.13	-0.0036
Region 5	0.00096	-0.00060	0.52	-0.0132

vations of these three datasets were also taken three times per month, corresponding with the soil moisture dataset after being binned in time. The numbers of stations at which precipitation and TDSA in each region were recorded are also listed in Table 1.

3. Tendency analysis

In this section, the statistical characteristics of soil moisture in different regions are first considered. The results of interannual and seasonal variations are also discussed. In order to discuss long-term variations of soil moisture, only those stations that could provide more than 10 years worth of data during the 18-year study period are used.

3.1 *Long-term trends and interannual variations*

To avoiding the effects of seasonal variations, the seasonal cycles of observations are firstly subtracted at every station. Figure 2 shows the 1981–1998 region-mean monthly soil moisture anomalies in the top 10-cm and 50-cm layers for the five regions. The time series of precipitation and TDSA anomalies for the same period in these five regions are shown in Fig. 3. A summary of linear trend coefficients for Figs. 2 and 3 are provided in Table 2.

Table 2 shows that the trends of soil moisture increased in the top 10-cm but decreased in the top 50-cm soil layers in most regions during this period. The trends of soil moisture in most regions are significant. Consistencies between the trends of soil moisture in the top 10-cm layer and precipitation can be seen for all five regions, particularly regions 2, 3, and 5, which show significant trends in precipitation. It is indicated that changes in precipitation might be one of the dominant factors affecting trends in soil moisture in the top 10-cm layer in these five regions of China.

Soil moisture in regions 2 and 4 show increasing trends for both layer depths, and the trend of soil moisture has a positive correlation with precipitation and a negative correlation with TDSA. In these two regions, the increasing trends of precipitation and de-

creasing trends of TDSA could have caused a positive trend in soil water storage. As changes in TDSA mainly affect evaporation from the land surface, this has a more marked effect on soil moisture in the top 10-cm layer than in deep layers. Therefore, the homothetic effects of increasing trends of precipitation and decreasing trends of TDSA are more pronounced in the top 10-cm layer, causing significant increasing trends of soil moisture in this area.

Decreasing trends in soil moisture can be seen for both layer depths in region 3, and the trend in deeper layers is much stronger. There are also downward trends in precipitation and TDSA. Notably, a downward trend in precipitation caused soil water content in both layer depths to decrease during this period. Decreasing trends in TDSA operate in a similar way to that of evaporation from the land surface. Therefore, to a certain extent, the positive effects of TDSA on soil moisture in surface layers can offset the negative effects of precipitation. In this way, the decreasing trend of the top 10-cm layer is weaker than that of the top 50-cm layer in this region.

In regions 1 and 5, the trends in soil moisture for both layer depths are not consistent with precipitation and TDSA, except for the trend of the top 10-cm layer in region 5. According to the analysis of Zhai et al. (1999), days during which extreme precipitation occurred over Northeast and Southwest China have decreased notably in the last 40 years. As soil moisture in deep layers are greatly influenced by the effects of extreme precipitation, one could suppose that the significant decreases in soil moisture in the top 50-cm layer might be a result of strong decreasing trends of extreme precipitation in these two regions.

3.2 *Seasonal variations*

Monthly and regional-mean seasonal cycles of soil moisture are presented in Figs. 4a and 4b. In all these regions, the monthly and regional means of soil moisture in the two layer depths almost show the same patterns of seasonal variation. However, considerable spatial heterogeneity of the means can also be seen.

Figures 4a and 4b show that among the five re-
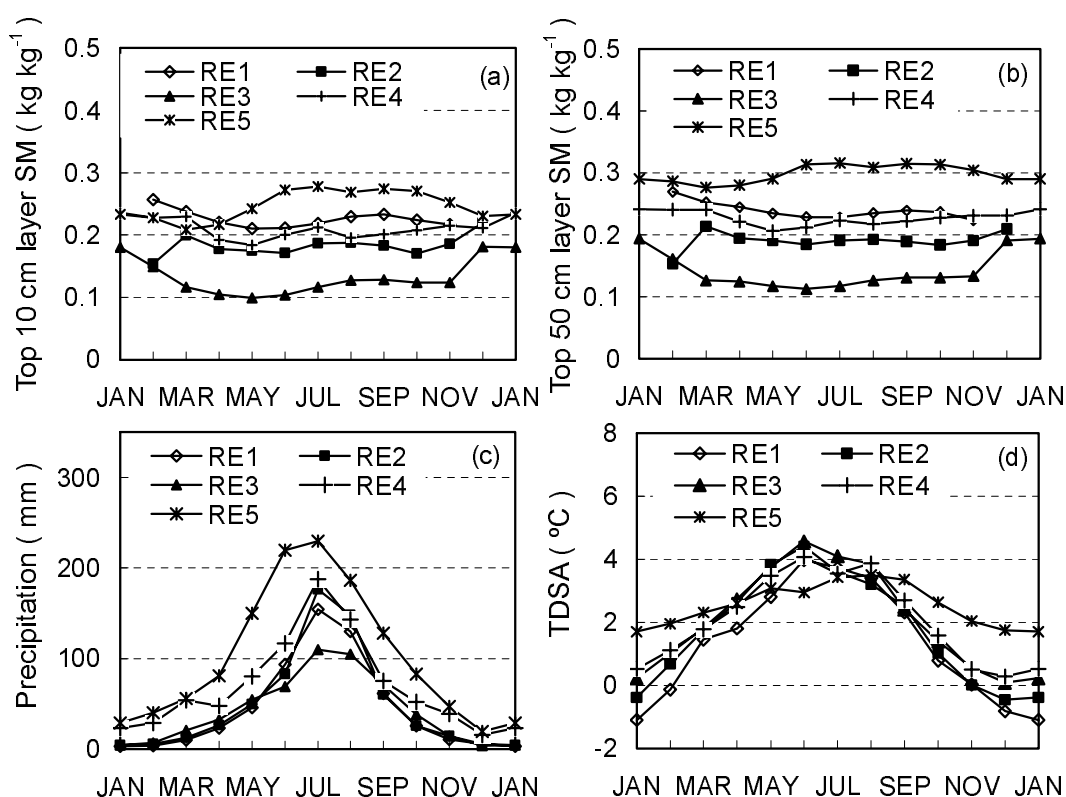
Fig. 4. Regional-mean seasonal cycles during the period 1981–1998 for the (a) top 10-cm layer soil moisture, (b) top 50-cm layer soil moisture, (c) precipitation, and (d) TDSA observations in region 1 to region 5.

gions, region 5 had the maximum soil moisture for both layer depths in most months of the year, while region 3 had the opposite. The other three regions had approximately similar soil moisture means for both layer depths across the entire year. The authors believe that region-dependent values of soil moisture in the two soil layer depths might be due to regional differences in precipitation. Figure 4c shows that regional differences in precipitation correspond to that of soil moisture, with region 5 having had the maximum value and region 3 the minimum. Regional differences of TDSA are not so distinct (Fig. 4d). Forepart from region 5, all other regions had similar seasonal cycles of TDSA. It is therefore suggested that regional variations in precipitation may be a major factor influencing regional differences in soil moisture in China.

Seasonal cycles of soil moisture means also show regional differences in China. Soil moisture in region 5 reaches a seasonal maximum in summer and then decreases slowly from autumn to winter. In spring it reaches a minimum for the year. In region 3, soil moisture remains in an almost stable state from spring through to fall. Following a quick increase from December, it reaches a seasonal high in winter. In the other three regions, seasonal variations in soil mois-

ture are weaker across the entire year.

In region 5, seasonal variation is strong for precipitation but weak for TDSA. With dominant effects of seasonal variation in precipitation, the seasonal cycle of soil moisture follows the cycle of precipitation well in this region. The case in region 3 is opposite to that of region 5. The variation of precipitation is gentle from spring to fall, but TDSA is in a high state during this period. With the influence of high TDSA, the supply of precipitation to soil water storage is less than the release of soil water by evaporation, which tends to cause soil moisture to be low. In winter, the lowest state of TDSA makes evaporation from soil water weaken. Furthermore, soil can be covered by snow during the winter, further retarding the motion of water out of the soil. Therefore, although precipitation is in a minimum state in winter, the effects of TDSA and snow cover can also cause soil moisture to be in its highest state in region 3. In three other regions, the influences of precipitation and TDSA on soil moisture might have a similar magnitude and reach a balance, making soil moisture maintain a stable state throughout the entire year.

It can be concluded that the seasonal variation in soil moisture in these regions is mainly controlled by

precipitation and evaporation. Soil moisture increases and is in a high state when precipitation is dominant, while it decreases and is in a low state when evaporation is dominant. In winter, snow cover might also have an important effect on the state of soil moisture.

4. Temporal scale analysis

Temporal scales and seasonal temporal scales of soil moisture and TDSA are analyzed in this section. Precipitation is a random and intermittent process, the temporal continuance of which is much shorter than that of soil moisture. According to the analysis of Skøien et al. (2003), the *e*-folding distance (the distance where the variable value is $1 - 1/e$ of its maximum value) of precipitation is in the order of one day. Therefore, the sampling interval (three times per month) of precipitation might not be dense enough to capture the temporal scale of precipitation here. For the limitation of precipitation data, only the temporal scales of soil moisture and TDSA are discussed in this section.

Although the dataset of soil moisture is binned to obtain standard time series for evaluating the temporal autocorrelation, the number of missing data is also large in every region. This causes difficulties in employing standard correlation analysis techniques. To estimate the autocorrelation coefficient with missing data, the method of Vinnikov and Yeserkepova (1991) was used.

4.1 *Temporal scale*

Delworth and Manabe (1988) developed a theory that soil moisture temporal variations correspond to the combination of a first-order Markov process signal and additive white noise by analyzing results from the Geophysical Fluid Dynamics Laboratory GCM. They assumed that the autocorrelation coefficient r has an exponential form:

$$r(t) = \begin{cases} 1 & \text{if} \quad t = 0 \,, \\ r_0 \exp\left(-\dfrac{t}{T}\right) & \text{if} \quad t \neq 0 \,, \end{cases} \quad (1)$$

where t is the time lag and T is the scale of temporal autocorrelation. The value of T has the meaning of the lag at which the autocorrelation is reduced to $1/e$. The parameter r_0 characterizes the part of the variance of red signal with autocorrelation. And $1 - r_0$ represents the variance of white noise components due to random processes. The theory was successfully applied for analyzing the temporal scales of soil moisture by Vinnikov et al. (1996) and Entin et al. (2000).

The seasonal cycles of soil moisture and TDSA were first subtracted from the observed values to cre-

ate anomalies, with which the autocorrelation functions were calculated. The seasonal variabilities of temporal scales will be discussed in the next subsection. For calculating autocorrelation coefficients, the smallest time lag used was 10 days, and the lag was increased to 4 months with 10-day increments. The natural logarithms of autocorrelation coefficients were plotted against the time lag to determine the temporal scale. The curves were truncated when the values of autocorrelation coefficients at the $n + 1$ time lags began to be greater than that at the n time lags. The estimates of autocorrelation coefficients of soil moisture and TDSA in every region are shown in Fig. 5. To determine the temporal scale of a region, the autocorrelation coefficients were averaged together, at each time lag value, and plotted along with a 95% confidence interval bracket. The linear lines that fitted through these values were the least squares fitting lines, the slopes of which are related to the temporal scales. The estimates of the temporal scale (T) and the ratio of the variance of red noise signal (r_0) of soil moisture and TDSA are summarized in Table 3.

Figure 5 shows that soil moisture fits each linear line well in every region, which indicates that the memory of soil moisture in both layers declined in exponential form. These results provide validation of the theory of Delworth and Manabe (1988) in the range of China. Table 3 indicates that timescales of soil moisture for both layers are roughly 1–3 months in all regions. Furthermore, there is a consistent increase in temporal scale with the increase of soil depth in every region. The timescale of TDSA has the same order of months as soil moisture. In most of these regions, it is smaller than the timescale of soil moisture.

Except for region 4, the temporal scale estimates of the other four regions increase slightly with depth, but the increments of red noise signal (r_0) are large enough. It is possible that the sampling interval (three times per month) used is not dense enough to capture enough white noise component in the top 10-cm layer and shifts the timescale into much longer values. Therefore, it reddens the spectrum of the temporal scale in the top 10-cm layer in these four regions and makes the spectrum closer to that of the deep layer.

There is a consistent increase in the variance of red signal in soil moisture with an increase in soil depth in every region, and the variance of the red noise signal of TDSA is smaller than that of soil moisture in both layers. The "red noise" signal in the Markov process embodies a correlation in time, while the "white noise" component represents a random variation that is independent of time. As soil in the top 10 cm is thin and interacts directly with the atmosphere, soil moisture in this layer can respond more sensitively to atmos-

Table 3. Estimates of the scales of temporal correlation T and the red noise component r_0 for soil moisture and TDSA in the five regions.

	0–10 cm soil moisture		0–50 cm soil moisture		TDSA	
	T (month)	r_0	T (month)	r_0	T (month)	r_0
Region 1	2.0	0.49	2.8	0.57	1.1	0.43
Region 2	2.4	0.44	2.6	0.57	1.7	0.38
Region 3	2.0	0.45	2.4	0.72	2.4	0.30
Region 4	1.8	0.43	3.4	0.56	1.1	0.42
Region 5	1.8	0.54	2.1	0.67	1.6	0.32
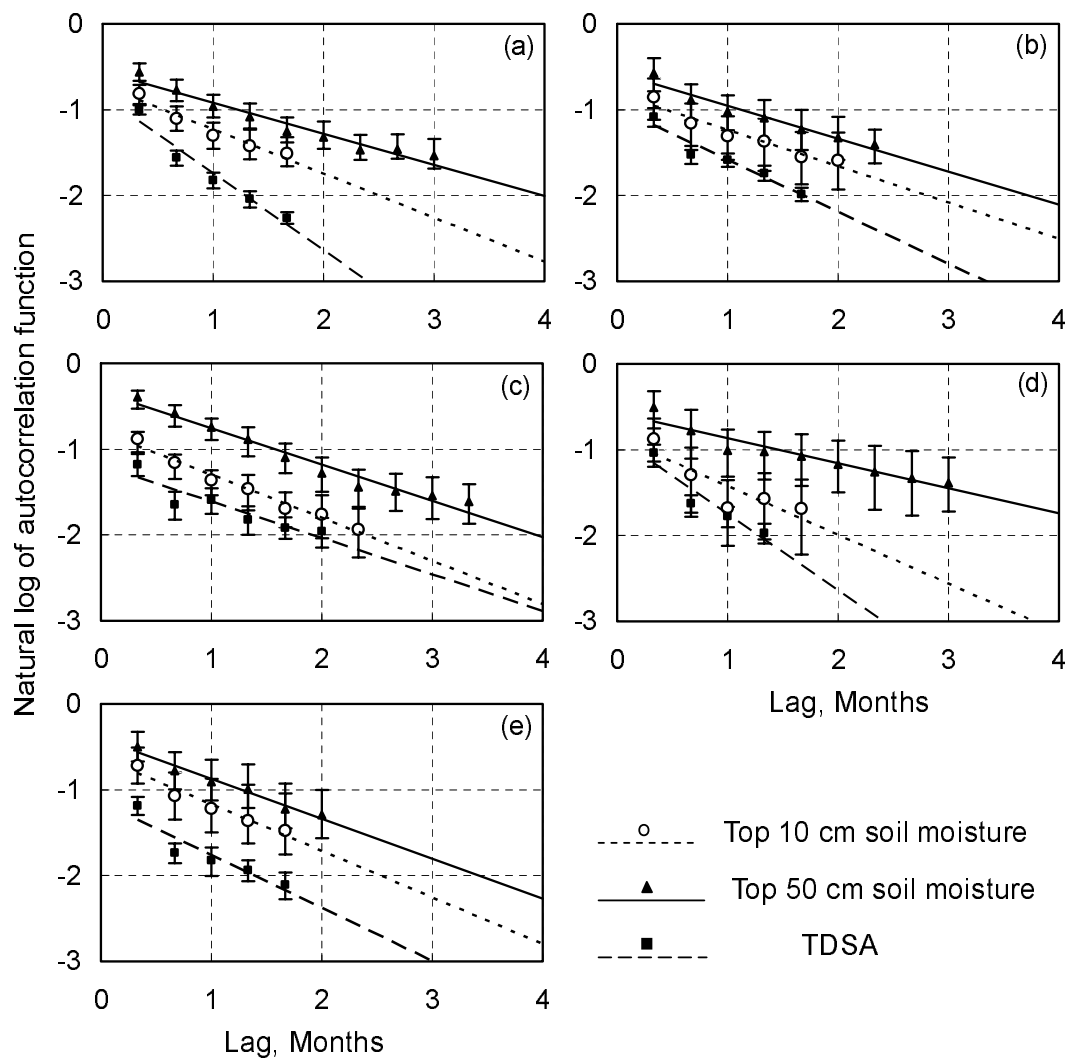
Fig. 5. Regional-mean temporal autocorrelation values and the least squares fitting lines of soil moisture in the two layers (circle points and short dashed lines for the top 10-cm layer; triangle points and solid lines for the top 50-cm layer) and TDSA (rectangle points and long dashed lines) for (a) region 1, (b) region 2, (c) region 3, (d) region 4, and (e) region 5. The error bars denote the 95% confidence interval for each mean point.

pheric forcing. Therefore, with the effect of a small red noise component in TDSA and a strong white noise component in precipitation, soil moisture in the surface layers has a corresponding smaller correlation in time than that in deeper layers. It is considered that as the water moves from the land surface to deep soil layers, the red noise component of soil water increases. Soil moisture imposes a longer memory on time variations with an increase in soil depth.

Entin et al. (2000) found that the temporal scale of soil moisture decreased in the direction of the equator. However, with more observations and a wider distribution of regions in this study, this rule cannot be found here. Region 5 is located in the lower latitudes, but the temporal scales of the top 50-cm soil layer in this region are larger than that in boreal regions. Region 2 does not have the highest latitude, but has the longest timescale in the top 10-cm soil layer. Combining soil texture, topography, vegetation and atmospheric forcing, a separation of timescales can be seen between those processes which affect temporal scales of soil moisture. All those factors change distinctly among different regions and affect soil moisture with different weights. With the influences of these factors, the spatial complexities of soil moisture timescales are much greater than previously thought.

4.2 Seasonal temporal scale

In addition to analyzing variation in the temporal scales of soil moisture, it is important to know how these scales vary during the year. The seasonal variations might explain other factors that might be missed in the annual analysis but can affect the overall scales.

For this analysis, the autocorrelation value of a given month is the correlation between the available observations of that month and the corresponding observations of the following month (i.e., r for May, lag one month, correlates with the values on 8, 18, 28 May, and 8, 18, 28 June respectively; then average these three values of r to obtain the correlation coefficient of May with one month lag; r for December with two months lag correlates the values in December and the values in February of the next year). To obtain the monthly temporal scale, the natural logarithm of the autocorrelation values for 1- and 2-month lags are calculated first. The monthly temporal scale would be equal to the inverse of the slope of the line that intersects both points. Since there are only two points, the scale for each month Tm can be determined by the following equation (Entin et al., 2000):

$$T_m = \frac{\ln(r_{m,2})}{\ln(r_{m,1})} , \qquad (2)$$

where m is the month for which the timescale is being

calculated, $r_{m,1}$ is the autocorrelation value between month m and month $m + 1$, and $r_{m,2}$ is the autocorrelation value between month m and month $m + 2$.

Figure 6 shows the seasonal timescale of soil moisture and TDSA. Because of the freezing season, there are no values in the winter for regions 1 and 2, which are located in the north of China. The missing values in other months are attributed to negative correlation coefficient values which cannot calculate natural logarithm values. The temporal scales of soil moisture are mainly 1–3 months in all regions during the entire year. Each region shows consistent seasonal variations in both two layer depths for timescales of soil moisture. However, the seasonal cycles of timescales are region-dependent. For example, in two boreal regions, regions 1 and 2, seasonal variations of timescale are gentle during the year, but regions 4 and 5 show clear seasonal cycles with two peaks in winter and summer respectively. The seasonal timescale of TDSA has the same order as that of soil moisture, but is not very consistent. As many other atmospheric forcings (e.g. precipitation and radiation) have strong influences on the state of soil moisture, seasonal variations of them and the weights of their influences on soil moisture can also affect variations in the "time memory" of soil moisture during the year. All these factors cause the complexities in seasonal variations of soil moisture timescales in all these regions.

5. Spatial scale analysis

The spatial scale is determined using a similar formula as the temporal scale. Using the data of all 103 non-irrigated soil moisture stations, the spatial variability scale of soil moisture in China are smaller than the maximum distance between any of the two observing stations in all regions. Therefore, the spatial scales of soil moisture are also analyzed in regions, as in previous sections. The correlation is preformed for each pair of stations in the same region and the correlation coefficient is plotted against the distance between the stations. The data are binned into different distance groups ranging from 50 km to about 800 km.

According to Vinnikov et al. (1996) and Entin et al. (2000), estimates of the spatial autocorrelation of the soil moisture field may be similar to the temporal autocorrelation. A logarithmic scale is also used here for spatial autocorrelation functions, as carried out earlier for temporal autocorrelation. The spatial autocorrelation coefficient r is also in exponential form:

$$r(l) = \begin{cases} 1 & \text{if } l = 0 , \\ r_0 \exp\left(-\dfrac{l}{L}\right) & \text{if } l \neq 0 , \end{cases} \qquad (3)$$
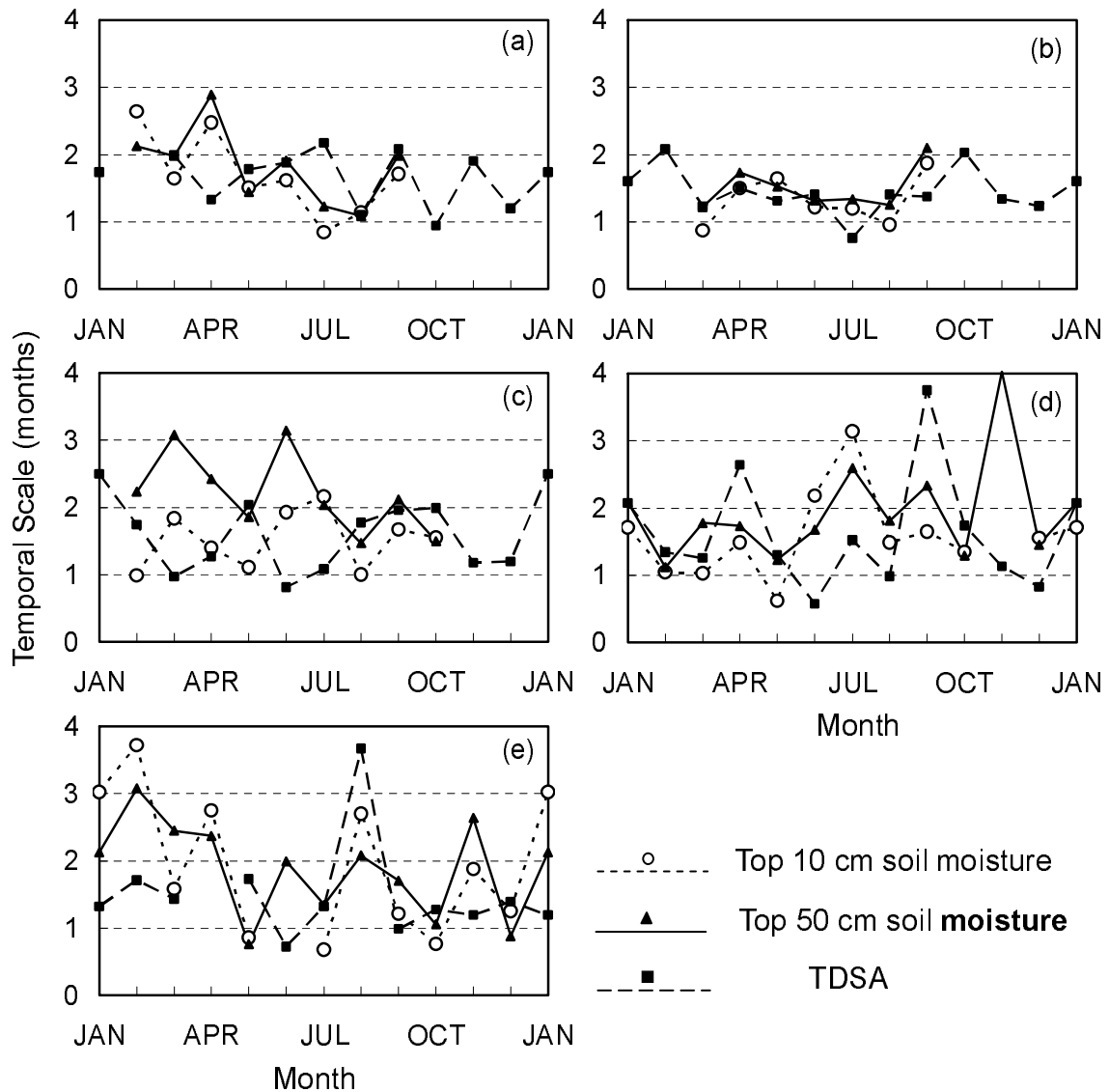
Fig. 6. Seasonal temporal scale of TDSA and soil moisture in the top 10-cm layer and 50-cm layer for (a) region 1, (b) region 2, (c) region 3, (d) region 4, and (e) region 5. The meaning of the points and lines are the same as for Fig. 5.

where l is the distance between stations, L represents the scale of spatial autocorrelation, and the parameter r_0 is the ratio of the variance of the red noise signal to the estimated variance. The mean correlation coefficient value is computed and then converted into natural logarithm values and plotted against the mean distance for each bin. Similarly, the spatial scales of precipitation and TDSA in these five regions are calculated with the same method as soil moisture.

5.1 *Spatial scale*

Figure 7 shows the spatial scales of soil moisture, precipitation, and TDSA in regions 1–5. The mean seasonal variation at each station is first subtracted.

The linear lines that fitted through these values were the least squares fitting lines of these points. The negative inverse of the slope of the fitting lines determine the spatial scales. Similar to the analysis of temporal scale in section 4, a summary of the estimates of spatial scales and the parameters r_0 is given in Table 4. The spatial scales of soil moisture range from 200–600 km within these regions. Furthermore, in all regions, the spatial scales of surface layers are larger than that of deeper layers. This result agrees with that of Liu et al. (2001), who used 99 stations in eastern China from 1987–1989. Similar to the changes in spatial scales with soil depth, the red noise component r_0 of spatial variability decrease corresponding to an in-
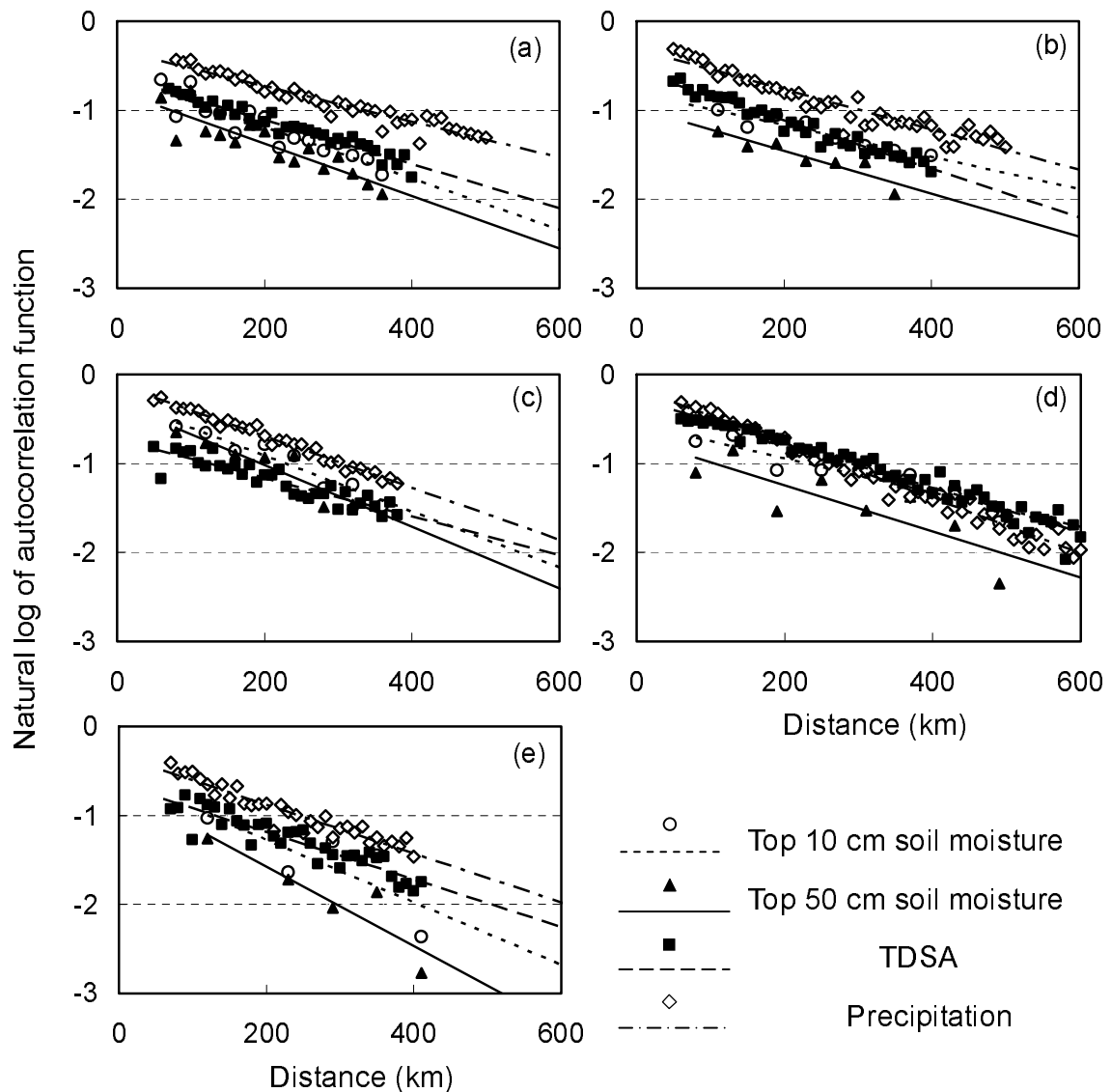
Fig. 7. Estimates of the spatial autocorrelation functions for soil moisture (circle points and short dashed lines for the top 10-cm layer; triangle points and solid lines for top-50 cm layer), TDSA (rectangle points and long dashed lines) and precipitation (diamond points and dash-dot lines) in (a) region 1, (b) region 2, (c) region 3, (d) region 4, and (e) region 5. The linear lines are the least squares fitting lines of corresponding points.

crease in depth. Vinnikov et al. (1996) assumed that the red noise component of spatial variability represented the statistical properties of monthly averaged precipitation fields, which embodied homogenous signals of spatial change, while the white noise component reflected an integration of random measurement errors and spatial heterogeneity in natural conditions around the measurement sites. Table 4 shows that precipitation has the biggest r_0 among other variables in all regions, which could verify the points made by Vinnikov et al. (1996). With a stronger influence of precipitation, much spatial homogeneity in signals of

precipitation can be easily transferred to soil moisture in the surface layer, causing a larger red noise component and spatial scales in this layer.

Table 4 also displays the effects of topography on the spatial scale of soil moisture. Spatial scales of two plain regions, regions 2 and 4, are larger than that of the other three mountainous regions. In plains, the mean slope is small. The movement of water in soil is weak in horizontal directions. Therefore, the spatial variation in soil moisture may follow the spatial patterns of precipitation and evaporation. According to the analysis in ection 4, the "time memory"

Table 4. Estimates of the spatial scale L and the red noise component r_0 for soil moisture in the top 10-cm layer and the top 50-cm layer, precipitation, and TDSA in regions 1 to 5. (Units of L: km)

| | Soil moisture | | | | Precipitation | | TDSA | |
| | Top 10 cm | | Top 50 cm | | | | | |
	L	r_0	L	r_0	L	r_0	L	r_0
Region 1	345	0.54	333	0.46	500	0.72	400	0.54
Region 2	556	0.45	417	0.38	370	0.78	370	0.57
Region 3	323	0.75	286	0.72	345	0.90	455	0.48
Region 4	588	0.55	479	0.44	323	0.86	400	0.76
Region 5	286	0.56	222	0.51	357	0.72	370	0.52

Table 5. Same as Table 4 except for each season in every region. (Units of L: km)

| | Winter | | Spring | | Summer | | Autumn | |
	L	r_0	L	r_0	L	r_0	L	r_0
Top 10 cm soil moisture								
RE 1	–	–	400	0.51	357	0.63	145	0.76
RE 4	769	0.51	–	–	357	0.66	500	0.74
Top 50 cm soil moisture								
RE 1	417	0.45	500	0.34	303	0.55	189	0.57
RE 4	555	0.47	–	–	400	0.44	417	0.67
Precipitation								
RE 1	526	0.90	625	0.95	556	0.80	–	–
RE 4	625	0.91	556	0.92	278	0.90	714	0.93
TDSA								
RE 1	400	0.58	909	0.71	625	0.62	–	–
RE 4	–	–	–	–	370	0.85	–	–

of soil moisture can hold for several months, while the "time memory" of precipitation is in the order of days (Skøien et al., 2003). With a strong memory in soil moisture, a sampling interval of a 10-day period can smooth out high frequency fluctuations in soil moisture in different stations and make it change in a similar fashion. In this way, the spatial scales of soil moisture in these two plain regions are large and also exceed that of precipitation and TDSA.

Unlike in plains, the patterns of precipitation and TDSA are obviously altered by mountains in regions 1, 3 and 5. Because a mountain between two stations decreases their correlation, the spatial scale of soil moisture is smaller than that in plains. Also, steep slopes in mountains make the water in soil move easily in horizontal directions. It reduces the "spatial memory" of soil moisture to precipitation and TDSA patterns and leads to the spatial scale of soil moisture being smaller than that of precipitation and TDSA.

5.2   *Seasonality of spatial scale*

Seasonality of spatial scale is analyzed in this subsection to find some features of spatial scale variations during the year. The conventional definitions for seasons are used: December, January and February for winter; March, April and May for spring, and so on. Because spatial scales of soil moisture cannot be obtained with data limitation in most seasons in regions 2, 3 and 5, seasonal spatial scales are only discussed in regions 1 and 4 here. Table 5 gives a summary of spatial scales and the parameter r_0 of soil moisture, precipitation and TDSA for different seasons in regions 1 and 4. The missing numbers in the table indicate not enough data in the season.

Similar to the analysis in the last subsection, the red noise component of soil moisture in the top 10-cm layer is larger than that of the top 50-cm layer in all seasons in these two regions. However, the spatial scales of the surface layer are not always larger than that of the deep layer. In the spring of region 1 and in the summer of region 4, soil moisture in the top 50-cm layer has larger spatial scales than that of the top 10-cm layer. Results indicate that although homogeneity of the signal embodied in the spatial change of soil moisture in the surface layer is larger than in the deep layer during the year, the effective impacts of the signal on the spatial scales of soil moisture varies with the seasons.

Table 5 also shows that the seasonal cycles of spatial scale of soil moisture in these two regions are dif-

ferent, whereas the seasonal variations of spatial scale in soil moisture are consistent with precipitation in each region. This indicates that the seasonal variations of spatial patterns in precipitation might be an important factor that affects the spatial scales of soil moisture.

6. Conclusions

Using the same methods as Entin et al. (2000) and Vinnikov et al. (1996) and a new soil moisture dataset in China, the long-term trends, seasonal variations, and the temporal and spatial scales of soil moisture in five different regions during 1981–1998 have been studied in detail. Three datasets of precipitation, land surface temperature, and air temperature were also used to analyze the underlying mechanisms of the characteristics of soil moisture. The major conclusions of this paper are as follows:

(1) In most regions, the trends of soil moisture in the top 10-cm layer were increasing while the trends in the top 50-cm layer were decreasing during the period 1981–1998. Changes in precipitation may be the dominant factor affecting the trends of soil moisture in both layer depths. The trend of TDSA has a secondary effect mainly on the trends of surface soil moisture. In regions 1 and 5, the trends of soil moisture in the deep layer may respond to the trends of extreme precipitation.

(2) Differences in soil moisture values between regions are clear. Region 5 has the maximum soil moisture and region 3 has the minimum during the entire year. The regional differences of precipitation may be a major factor that causes the area differentiation of soil moisture in China. The seasonal cycles of soil moisture means also have regional differences. The seasonal variations of soil moisture are mainly controlled by precipitation and evaporation. Soil moisture increases when precipitation is dominant and decreases when evaporation is dominant. In winter, snow cover might also have an important effect on the state of soil moisture.

(3) Timescales of soil moisture in both two layer depths are roughly 1–3 months in all regions, and the timescale of TDSA has the same order of months as soil moisture.

(4) There is a consistent increase in temporal scale and the red signal of soil moisture with an increase in soil depth. The variance of red noise signal of TDSA is smaller than that of soil moisture. A corresponding small correlation in time of soil moisture in the surface layer may be a result of effects of a small red noise component in TDSA and a strong white noise component in precipitation.

(5) The timescale of soil moisture has consistent seasonal variations for both two layer depths in all regions, and seasonal cycles of timescales are region-dependent. The seasonal variations of TDSA cannot be satisfactorily consistent with that of soil moisture. The authors guess that other atmospheric forcings (e.g. precipitation and radiation) may have a strong influence on the variations of "time memory" of soil moisture during the entire year.

(6) The spatial scales of soil moisture in all the regions are in the order of hundreds of kilometers, ranging from 200–600 km. Furthermore, the spatial scales of the surface layer are larger than that of the deep layer. With a stronger influence of precipitation, much spatial homogeneity in the signal of this can be easily transferred to soil moisture in the surface layer, causing a large red noise component and spatial scale in this layer.

(7) Topography also has some effects on the spatial scale of soil moisture. Spatial scales of soil moisture in plains are larger than that of mountainous areas. In plains, the spatial scale of soil moisture mainly follows the spatial patterns of precipitation and evaporation. With a strong time memory in soil moisture, the sampling interval of 10 days can smooth out the high frequency fluctuations of this, making it change in a similar fashion. In mountain areas, mountainous topography reduces the spatial memory of soil moisture to precipitation patterns and leads to a smaller spatial scale than in plains.

(8) The seasonal variations in spatial scales of soil moisture are consistent with those of precipitation. The authors believe that the seasonal variations in spatial patterns of precipitation might be an important factor affecting the spatial scales of soil moisture in different regions of China.

Land surface states are a strong nonlinear system, and there might be strong nonlinear interactions with mesoscale atmospheric circulations that feed back on the soil moisture. The feedback action between soil moisture and atmospheric processes can be studied in the future with higher resolution soil moisture observation datasets and meteorological fields.

Although a new dataset of soil moisture has been studied, there are still very little data in the west of China included in this research. However, the climatology of the west of China, particularly the Tibetan Plateau, is distinctly different from that in the east of the country. The climatology and scales of soil moisture in the west of China should be studied with more data in this area in the future.

REFERENCES

Cayan, D. R., and K. P. Georgakakos, 1995: Hydroclimatology of continental watersheds, 2, spatial analyses. *Water Resour. Res.*, **31**, 677–698.

Dai A. G., K. E. Trenberth, and T. T. Qian, 2004: A global dataset of Palmer severity index for 1870–2002: Relationship with soil moisture and effects of surface warming. *Journal of Hydrometeorology*, **5**, 1117–1130.

Delworth, T., and S. Manabe, 1988: The influence of potential evaporation on the variabilities of simulated soil wetness and climate. *J. Climate*, **1**, 523–547.

Dirmeyer, P. A., 2000: Using a global soil wetness dataset to improve seasonal climate simulation. *J. Climate*, **13**, 2900–2922.

Entin, J., A. Robock, K. Y. Vinnikov, V. Zabelin, S. Liu, A. Namkhai, and T. Adyasuren, 1999: Evaluation of Global Soil Wetness Project soil moisture simulations. *J. Meteor. Soc. Japan*, **77**, 183–198.

Entin, J., A. Robock, K. Y. Vinnikov, S. E. Hollinger, S. Liu, and A. Namkai, 2000: Temporal and spatial scales of observed soil moisture variations in the extratropics. *J. Geophys. Res.*, **105**, 11865–11877.

Fast, J. D., and M. D. McCorcle, 1991: The effect of heterogeneous soil moisture on a summer baroclinic circulation in the central United States. *Mon. Wea. Rev.*, **119**, 2140–2167.

Koster, R. D., and M. J. Suarez, 1995: Relative contributions of land and ocean processes to precipitation variability. *J. Geophys. Res.*, **100**, 13775–13790.

Koster, R. D., and M. J. Suarez, 1996: The influence of land surface moisture retention on precipitation statistics. *J. Climate*, **9**, 2551–2567.

Koster, R. D., M. J. Suarez, and M. Heiser, 2000: Variance and predictability of precipitation at seasonal-to-interannual timescales. *Journal of Hydrometeorology*, **1**, 26–46.

Koster, R. D., and Coauthors, 2004: Regions of strong coupling between soil moisture and precipitation. *Science*, **305**, 1138–1140.

Li, H. B., A. Robock, S. X. Liu, X. G. Mo, and P. Viterbo, 2005: Evaluation of reanalysis soil moisture simulations using updated Chinese soil moisture observations. *Journal of Hydrometeorology*, **6**, 180–193.

Liu, S. X., X. G. Mo, H. B. Li, G. B. Peng, and A. Robock, 2001: Spatial variation of soil moisture in China: Geostatistical characterization. *J. Meteor. Soc. Japan*, **79**, 555–574.

Robock, A., K. Y. Vinnikov, C. A. Schlosser, N. A. Speranskaya, and Y. Xue, 1995: Use of midlatitude soil moisture and meteorological observations to validate soil moisture simulations with biosphere and bucket models. *J. Climate*, **8**, 15–35.

Robock, A., K. Y. Vinnikov, and A. Schlosser, 1997: Evaluation of land-surface parameterization schemes using observations. *J. Climate*, **10**, 377–379.

Robock, A., C. A. Schlosser, K. Y. Vinnikov, N. A. Speranskaya, and J. K. Entin, 1998: Evaluation of AMIP soil moisture simulations. *Global and Planetary Change*, **19**, 181–208.

Robock, A., K. Y. Vinnikov, G. Srinivasan, J. K. Entin, S. E. Hollinger, N. A. Speranskaya, S. X. Liu, and A. Namkhai, 2000: The Global Soil Moisture Data Bank. *Bull. Amer. Meteor. Soc.*, **81**, 1281–1299.

Schlosser, C. A., A. Robock, K. Y. Vinnikov, N. A. Speranskaya, and Y. K. Xue, 1997: 18-year land-surface hydrology model simulations for a midlatitude grassland catchment in Valdai, Russia. *Mon. Wea. Rev.*, **125**, 3279–3296.

Schlosser, C. A., and Coauthors, 2000: Simulations of a boreal grassland hydrology at Valdai, Russia: PILPS Phase 2(d). *Mon. Wea. Rev.*, **128**, 301–321.

Shinoda, M., and Y. Yamaguchi, 2003: Influence of soil moisture anomaly on temperature in the Sahel: A comparison between wet and dry decades. *Journal of Hydrometeorology*, **4**, 437–447.

Shukla, J., and Y. Mintz, 1982: Influence of land-surface evapotranspiration on the earth's climate. *Science*, **215**, 1498–1501.

Skøien, J. O., G. Blöschl, and A. W. Western, 2003: Characteristic space scales and timescales in hydrology. *Water Resour. Res.*, **39**(10), 1304.

Srinivasan, G., and Coauthors, 2000: Soil moisture simulations in revised AMIP models. *J. Geophys. Res.*, **105**, 26635–26644.

Timbal, B., S. Power, R. Colman, J. Viviand, and S. Lirola, 2002: Does soil moisture influence climate variability and predictability over Australia? *J. Climate*, **15**, 1230–1238.

van den Hurk, B. J. J. M., W. G. M. Bastiaanssen, H. Pelgrum, and E. van Meijgaard, 1997: A new methodology for assimilation of initial soil moisture fields in weather prediction models using meteosat and NOAA data. *J. Appl. Meteor.*, **36**, 1271–1283.

Vinnikov, K. Y., and I. B. Yeserkepova, 1991: Soil moisture: Empirical data and model results. *J. Climate*, **4**, 66–79.

Vinnikov, K. Y., A. Robock, N. A. Speranskaya, and C. A. Schlosser, 1996: Scales of temporal and spatial variability of midlatitude soil moisture. *J. Geophys. Res.*, **101**, 7163–7174.

Vinnikov, K. Y., A. Robock, S. Qiu, and J. K. Entin, 1999a: Optimal design of surface networks for observation of soil moisture. *J. Geophys. Res.*, **104**, 19743–19750.

Vinnikov, K. Y., A. Robock, S. Qiu, J. K. Entin, M. Owe, B. J. Choudhury, S. E. Hollinger, and E. G. Njoku, 1999b: Satellite remote sensing of soil moisture in Illinois, United States. *J. Geophys. Res.*, **104**, 4145–4168.

Zhai, P., F. M. Ren, and Q. Zhang, 1999: Detection of trends in China's precipitation extremes. *Acta Meteorologica Sinica*, **57**, 208–216. (in Chinese)

Zhang, X. Z., X. Y. Wu, and J. He, 2004: Vertical character of soil moisture in China. *Acta Meteorologica Sinica.*, **62**, 51–61. (in Chinese)